

Research of Shielding Effectiveness of Metallic Experiment Box Based on Modal Method of Moments

Guishu Xia, Chao Zhou

Aviation Engineering Institute, Civil Aviation Flight University of China, Guanghan Sichuan 618307, China

Abstract—In this paper, electric field shielding effectiveness (SE) of metallic experiment box with apertures illuminated by vertical polarization plane wave has been studied by using modal method of moment technique. Electric field SE has been calculated at three different points on the same plane inside enclosure. The numerical results of the proposed technique are in very good agreement with data available in the literature and experimental results. It is shown that apertures' position, aperture' number and calculation points have noticeable effect on the electric field SE, four apertures is a better select to improve the shielding ability of an enclosure than one aperture while they have the same area.

Keywords—Rectangular enclosure, Apertures, SE, MoM, Green's function

I. INTRODUCTION

Metallic shielding enclosures are frequently employed to protect against radiation from both external EM fields and electromagnetic leakage from interior components. However, the integrity of these enclosures is often compromised by apertures of various sizes and shapes used to accommodate visibility, ventilation or access to interior components. Since these apertures at appropriate electromagnetic frequencies behave as very efficient antennas, they also become sources of electromagnetic interference problems for both EM emission and susceptibility. So it is very important to know the SE of shielding enclosures in the presence of these apertures. Several analytical and numerical techniques to estimate SE of metallic enclosures with apertures have been suggested in past years. Robinson et al. [1], [2] introduced a very simple analytical method based on transmission line model. However, this approach is limited by the assumption of thin apertures, simple geometries, negligible mutual coupling between apertures and fields can be calculated only at points in front of the aperture. In past years, some numerical techniques have been applied to the analysis of shielding effectiveness, such as finite difference time domain (FDTD) [3][4], finite element method (FEM) [5][6], method of moments (MoM) [7][8], transmission line matrix (TLM) [9][10] and hybrid method[11] are utilised with good accuracy over a broad frequency band at the cost of large amount of computer memory and CPU time. Deshpande introduced a moment method technique(modal MoM) using entire domain basis functions to represent apertures fields and therefore the magnetic currents on the apertures, which can evaluates the SE of a zero thickness enclosure exposed to a normally incident plane wave accurately at the center inside enclosure[12]. Nowadays the EM shielding effectiveness has becoming a hot research area in electromagnetic compatibility.

II. ELECTROMAGNETIC PROBLEM AND THE FORMULATION OF MODAL MoM

The shielding effectiveness of an enclosure is defined as

$$SE(dB) = -20 \log \left(\frac{|E_{int}|}{|E_{ext}|} \right) \quad (1)$$

where E_{int} is the electric field at a given point inside the enclosure, E_{ext} is the electric field at the same point in the absence of the enclosure. Therefore, the problem of SE estimation is essentially the problem of calculating the cavity fields excited by a plane wave incident from free space upon shielding enclosure.

Fig. 1 shows a rectangular enclosure with rectangular apertures exposed to a normal incident plane wave. The dimensions of the cavity are $a \times b \times c$. There are r number of apertures and the dimensions of the r th aperture are $L_r \times W_r$. The orientation of reference axes is also shown with origin at the lower right corner of front wall.

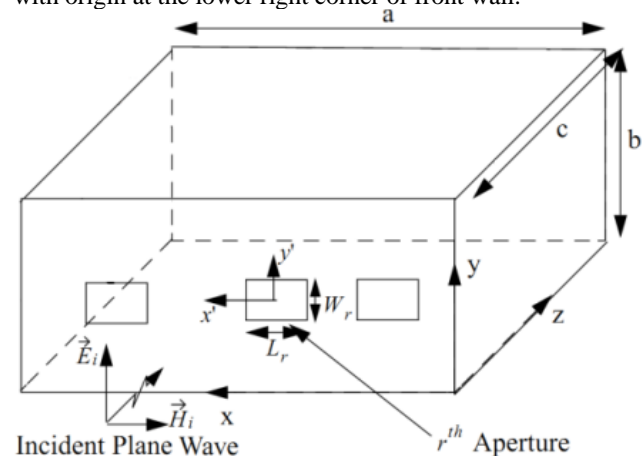


Figure1. Geometry of rectangular enclosure with rectangular apertures exposed to a normal incident plane wave

In modal MoM formulation, we assume that apertures are relatively small compared to walls in which they are located and are placed far enough away from the edges of enclosure. In addition, the edge diffracted fields are neglected. These assumptions enable us to use image theory and equivalence principles, surface equivalence principle. The apertures both internal (Region II) and external (Region I) to the enclosure can be replaced by equivalent magnetic currents of

$$M = n \times E_{apt} \quad (2)$$

Where E_{apt} is the tangential electric field induced on the apertures and n is the aperture normal vector.

$$\mathbf{E}_{apt}(z=0) = \sum_{r=1}^R \left[\hat{y} \sum_p \sum_q U_{rpq} \sin\left(\frac{p\pi}{L_r}\left(\frac{L_r}{2} + x - x_{cr}\right)\right) \times \cos\left(\frac{q\pi}{W_r}\left(\frac{W_r}{2} + y - y_{cr}\right)\right) + \hat{x} \sum_p \sum_q V_{rpq} \cos\left(\frac{p\pi}{L_r}\left(\frac{L_r}{2} + x - x_{cr}\right)\right) \times \sin\left(\frac{q\pi}{W_r}\left(\frac{W_r}{2} + y - y_{cr}\right)\right) \right] \quad (3)$$

Where U_{rpq} and V_{rpq} are unknown amplitudes of pq th mode of magnetic current on the outer of r th aperture that are non-zero at the aperture and zero elsewhere. L_r and W_r are the length and width of r th aperture, x_{cr} and y_{cr} are center coordinates of r th aperture. \hat{x} , \hat{y} are unit vectors in x , y directions. The unknown amplitudes U_{rpq} , V_{rpq} are determined by setting up coupled integral equations.

Using equivalence principle, equivalent magnetic currents are

$$\begin{aligned} \mathbf{M}_{apt} &= \mathbf{n}_1 \times \mathbf{E}_{apt} = -\hat{z} \times \mathbf{E}_{apt}(z=0) \\ &= \sum_{r=1}^R [\hat{x} \sum_p \sum_q U_{rpq} \Psi_r - \hat{y} \sum_p \sum_q V_{rpq} \Phi_r] \\ &= \sum_{r=1}^R \mathbf{M}_{r1} \end{aligned} \quad (4)$$

Where

$$\Psi_r = \sin\left(\frac{p\pi}{L_r}\left(\frac{L_r}{2} + x - x_{cr}\right)\right) \times \cos\left(\frac{q\pi}{W_r}\left(\frac{W_r}{2} + y - y_{cr}\right)\right) \quad (5)$$

$$\Phi_r = \cos\left(\frac{p\pi}{L_r}\left(\frac{L_r}{2} + x - x_{cr}\right)\right) \times \sin\left(\frac{q\pi}{W_r}\left(\frac{W_r}{2} + y - y_{cr}\right)\right) \quad (6)$$

Consider the aperture on $z=0$ plane, scattered EM field outside due to r th aperture can be determined by solving electric vector potential

$$\mathbf{E} = -\frac{1}{\epsilon_0} \nabla \times \mathbf{F} \quad (7)$$

$$\mathbf{H} = -\frac{j\omega}{k_0^2} (\nabla \nabla \cdot \mathbf{F} - \nabla^2 \mathbf{F}) \quad (8)$$

Where electric vector potential \mathbf{F} is given by

$$\mathbf{F} = \frac{\epsilon_0}{4\pi} \iint_{apt} 2\mathbf{M}_r \frac{e^{-jk_0|\mathbf{r}-\mathbf{r}'|}}{\mathbf{r}-\mathbf{r}'} d\mathbf{s} \quad (9)$$

Superposition of scattered electromagnetic field due to all apertures on $z=0$ plane gives the total scattered field as [12]

$$\begin{aligned} H_x^I &= \sum_{r=1}^R \sum_p \sum_q \frac{\omega \epsilon_0}{4\pi^2 k_0^2} (U_{rpq} \int_{-\infty}^{\infty} \int_{-\infty}^{\infty} e^{-jk_z|z-z'|} \Psi_{rpqy} \times \\ &\quad \frac{k_0^2 - k_z^2}{k_z} e^{jk_x x + jk_y y} dk_x dk_y - V_{rpq} \int_{-\infty}^{\infty} \int_{-\infty}^{\infty} e^{-jk_z|z-z'|} \times \\ &\quad \Phi_{rpqy} \frac{-k_x k_y}{k_z} e^{jk_x x + jk_y y} dk_x dk_y) \end{aligned} \quad (10)$$

$$\begin{aligned} H_y^I &= \sum_{r=1}^R \sum_p \sum_q \frac{-\omega \epsilon_0}{4\pi^2 k_0^2} (V_{rpq} \int_{-\infty}^{\infty} \int_{-\infty}^{\infty} e^{-jk_z|z-z'|} \Phi_{rpqy} \times \\ &\quad \frac{k_0^2 - k_y^2}{k_z} e^{jk_x x + jk_y y} dk_x dk_y - U_{rpq} \int_{-\infty}^{\infty} \int_{-\infty}^{\infty} e^{-jk_z|z-z'|} \times \\ &\quad \Psi_{rpqy} \frac{-k_x k_y}{k_z} e^{jk_x x + jk_y y} dk_x dk_y) \end{aligned} \quad (11)$$

$$\begin{aligned} H_z^I &= \sum_{r=1}^R \sum_p \sum_q \frac{-\omega \epsilon_0}{4\pi^2 k_0^2} \left(\int_{-\infty}^{\infty} \int_{-\infty}^{\infty} e^{-jk_z|z-z'|} (U_{rpq} \Psi_{rpqy} k_x \right. \\ &\quad \left. - V_{rpq} \Phi_{rpqy} k_y) e^{jk_x x + jk_y y} dk_x dk_y \right) \end{aligned} \quad (12)$$

In expressions (10)-(12) Φ_{rpqy} is Fourier transform of Φ_{rpqy} and Ψ_{rpqy} is Fourier transform of Ψ_{rpqy} .

The equivalent magnetic currents, present on the apertures of the enclosure, radiate electromagnetic fields inside the enclosure. The total electromagnetic field at any point inside enclosure is obtained by a superposition of fields due to each equivalent magnetic current source. considering x -component of magnetic current and using dyadic Green's function, The total magnetic field inside the enclosure is then obtained from [12] as

$$\begin{aligned} H_x^{IIx0} &= \frac{-j\omega}{k_0^2} \sum_{r=1}^R \sum_{p,q} U_{rpq} \sum_{m,n} \frac{-\epsilon_0}{k_l} \frac{\epsilon_{0m} \epsilon_{0n}}{ab \sin(k_l c)} \\ &\quad \times \left(k_0^2 - \left(\frac{m\pi}{a}\right)^2 \right) \sin\left(\frac{m\pi x}{a}\right) \\ &\quad \times \cos\left(\frac{n\pi y}{b}\right) \cos(k_l(z-c)) I_{rpqmnx} \end{aligned} \quad (13)$$

$$\begin{aligned} H_y^{IIx0} &= \frac{-j\omega}{k_0^2} \sum_{r=1}^R \sum_{p,q} U_{rpq} \sum_{m,n} \frac{-\epsilon_0}{k_l} \frac{\epsilon_{0m} \epsilon_{0n}}{ab \sin(k_l c)} \\ &\quad \times \frac{m\pi}{a} \left(-\frac{n\pi}{b}\right) \cos\left(\frac{m\pi x}{a}\right) \\ &\quad \times \sin\left(\frac{n\pi y}{b}\right) \cos(k_l(z-c)) I_{rpqmny} \end{aligned} \quad (14)$$

$$\begin{aligned} H_z^{IIx0} &= \frac{-j\omega}{k_0^2} \sum_{r=1}^R \sum_{p,q} U_{rpq} \sum_{m,n} \frac{-\epsilon_0}{k_l} \frac{\epsilon_{0m} \epsilon_{0n}}{ab \sin(k_l c)} \\ &\quad \times \frac{m\pi}{a} (-k_l) \cos\left(\frac{m\pi x}{a}\right) \\ &\quad \times \cos\left(\frac{n\pi y}{b}\right) \sin(k_l(z-c)) I_{rpqmny} \end{aligned} \quad (15)$$

In (13)-(15),

$$I_{rpqmny} = \iint_q \Psi_{rpqx}(x', y') \sin\left(\frac{m\pi x'}{a}\right) \cos\left(\frac{n\pi y'}{b}\right) dx' dy'$$

Likewise, considering y -component of magnetic current and using proper boundary conditions, The total magnetic field inside the enclosure is then obtained from [12] as

$$\begin{aligned} H_x^{IIy0} &= \frac{-j\omega}{k_0^2} \sum_{r=1}^R \sum_{p,q} -V_{rpq} \sum_{m,n} \frac{-\epsilon_0}{k_l} \frac{\epsilon_{0m} \epsilon_{0n}}{ab \sin(k_l c)} \\ &\quad \times \left(-\frac{m\pi}{a}\right) \frac{n\pi}{b} \sin\left(\frac{m\pi x}{a}\right) \cos\left(\frac{n\pi y}{b}\right) \times \cos(k_l(z-c)) I_{rpqmny} \end{aligned} \quad (16)$$

$$\begin{aligned} H_y^{IIy0} &= \frac{-j\omega}{k_0^2} \sum_{r=1}^R \sum_{p,q} -V_{rpq} \sum_{m,n} \frac{-\epsilon_0}{k_l} \frac{\epsilon_{0m} \epsilon_{0n}}{ab \sin(k_l c)} \\ &\quad \times \left(k_0^2 - \left(\frac{n\pi}{b}\right)^2 \right) \cos\left(\frac{m\pi x}{a}\right) \times \sin\left(\frac{n\pi y}{b}\right) \cos(k_l(z-c)) I_{rpqmny} \end{aligned} \quad (17)$$

$$H_z^{IIy0} = \frac{-j\omega}{k_0^2} \sum_{r=1}^R \sum_{p,q} -V_{rpq} \sum_{m,n} \frac{-\epsilon_0}{k_l} \frac{\epsilon_{0m} \epsilon_{0n}}{ab \sin(k_l c)}$$

$$\times \frac{n\pi}{b} (-k_l) \cos\left(\frac{m\pi x}{a}\right) \times \cos\left(\frac{n\pi y}{b}\right) \sin(k_l(z - c)) I_{rpqmn} \quad (18)$$

For a unique solution the electromagnetic fields in various regions satisfy continuity conditions over their common surfaces. The tangential electric fields over the apertures are continuous. The tangential magnetic over the apertures must also be continuous, thus yielding coupled integral equations with the magnetic currents as known variables. The coupled integral equation in conjunction with the method of moments can be solved for the amplitudes of magnetic currents. The total tangential fields inside the cavity from apertures are written as

$$\mathbf{H}_x^{\text{II}} = \mathbf{H}_x^{\text{II}x0} + \mathbf{H}_x^{\text{II}y0} \quad (19)$$

$$\mathbf{H}_y^{\text{II}} = \mathbf{H}_y^{\text{II}x0} + \mathbf{H}_y^{\text{II}y0} \quad (20)$$

Applying the continuity of tangential magnetic field on $z=0$ plane yields

$$\mathbf{H}_x^{\text{I}}|_{z=0} + \mathbf{H}_{xi}|_{z=0} = \mathbf{H}_x^{\text{II}}|_{z=0} \quad (21)$$

$$\mathbf{H}_y^{\text{I}}|_{z=0} + \mathbf{H}_{yi}|_{z=0} = \mathbf{H}_y^{\text{II}}|_{z=0} \quad (22)$$

Now selecting $\Psi_{r'p'q'x}$ as a testing function and use of Galerkin's method reduces the (21) to

$$I_{r'p'q'xi} = \sum_{r=1}^R \sum_{p,q} (U_{rpq} Y_{rpqr'p'q'}^{x1x1} + V_{rpq} Y_{rpqr'p'q'}^{x1y1}) \quad (23)$$

where

$$Y_{rpqr'p'q'}^{x1x1} = \frac{-j\omega}{k_0^2} \sum_{m,n=0}^{\infty} \frac{-\varepsilon_0}{k_l} \frac{\varepsilon_{0m}\varepsilon_{0n}}{ab \sin(k_l c)} \times (k_0^2 - \left(\frac{m\pi}{a}\right)^2) \cos(k_l c) I_{rpqmn} I_{r'p'q'mnx} \quad (24)$$

$$Y_{rpqr'p'q'}^{x1y1} = \frac{j\omega}{k_0^2} \sum_{m,n=0}^{\infty} \frac{-\varepsilon_0}{k_l} \frac{\varepsilon_{0m}\varepsilon_{0n}}{ab \sin(k_l c)} \left(\frac{m\pi}{a}\right) \left(\frac{n\pi}{b}\right) \times \cos(k_l c) I_{rpqmn} I_{r'p'q'mny} \quad (25)$$

$$I_{r'p'q'xi} = \iint_{r'p'q'} \mathbf{H}_{xi} \Psi_{r'p'q'x} dxdy \quad (26)$$

Similarly, selecting $-\Phi_{r'p'q'y}$ as a testing function and use of Galerkin's method reduces the (22) to

$$I_{r'p'q'yi} = \sum_{r=1}^R \sum_{p,q} (U_{rpq} Y_{rpqr'p'q'}^{y1x1} + V_{rpq} Y_{rpqr'p'q'}^{y1y1}) \quad (27)$$

where

$$Y_{rpqr'p'q'}^{y1x1} = \frac{j\omega}{k_0^2} \sum_{m,n=0}^{\infty} \frac{-\varepsilon_0}{k_l} \frac{\varepsilon_{0m}\varepsilon_{0n}}{ab \sin(k_l c)} \left(\frac{m\pi}{a}\right) \left(-\frac{n\pi}{b}\right) \times \cos(k_l c) I_{rpqmn} I_{r'p'q'mny} \quad (28)$$

$$\frac{\omega\varepsilon_0}{4\pi^2 k_0^2} \int_{-\infty}^{+\infty} \int_{-\infty}^{+\infty} \Phi_{rpqy} \Phi_{r'p'q'y}^* \frac{(k_0^2 - k_x^2)}{k_z} dk_x dk_y \quad (29)$$

$$I_{r'p'q'yi} = \iint_{r'p'q'} \mathbf{H}_{yi} \Phi_{r'p'q'y} dxdy \quad (30)$$

Equation (23) and (27) can be written in a matrix form as

$$\begin{bmatrix} Y_{rpqr'p'q'}^{x1x1} & Y_{rpqr'p'q'}^{x1y1} \\ Y_{rpqr'p'q'}^{y1x1} & Y_{rpqr'p'q'}^{y1y1} \end{bmatrix} \begin{bmatrix} U_{rpq} \\ V_{rpq} \end{bmatrix} = \begin{bmatrix} I_{r'p'q'xi} \\ 0 \end{bmatrix} \quad (31)$$

The matrix equation (31) can be numerically solved for the unknown amplitudes of equivalent magnetic currents induced on the apertures due to given incident field. From the knowledge of these amplitudes electromagnetic field inside as well as outside the enclosure can be obtained.

III. RESULTS AND DISCUSSION

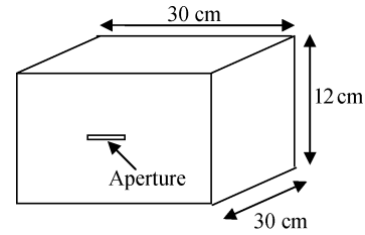


Figure 2. Geometry of 30 cm × 12 cm × 30 cm enclosure with a single aperture at (15 cm, 6 cm, 0)

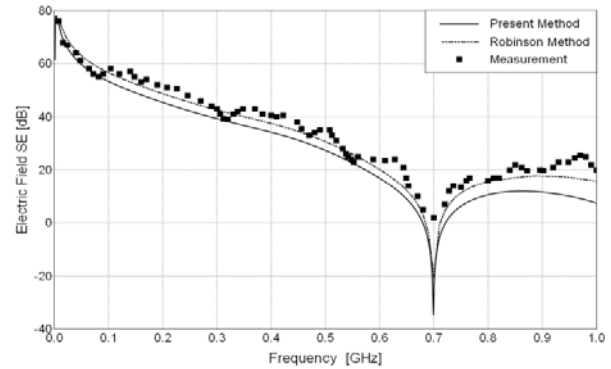


Figure 3. Electric field SE calculated at the center of 30 cm × 12 cm × 30 cm enclosure with 10 cm × 0.5 cm aperture located at 15 cm × 6 cm in $z=0$ plane with dominant cavity mode considered.

Firstly, we consider a rectangular enclosure of size (30 cm × 12 cm × 30 cm) with a rectangular aperture of size (10 cm × 0.5 cm) located at the center of the front wall (15 cm, 6 cm, 0) for the validation of present technique, as illustrated in Fig. 2. The enclosure is illuminated by a normal incident plane wave at 0 polarization. Assuming only expansion mode on the aperture and considering only dominant mode inside the enclosure. SE is calculated at the center of the enclosure. electric field SE obtained using expression (35) is plotted in Figure 4 along with the results from [2]. It is observed that numerical data obtained using present method agrees well with the earlier published results. Experimental data from [2] is also reproduced in Fig. 3.

Secondly, in order to study the electric field shielding of different points in the cavity, the same geometry with Figure 2 is selected. The enclosure is illuminated by a normal

incident plane wave at 0 polarization. The shielding effectiveness with dominant cavity mode considered is also calculated at many different points in the cavity.

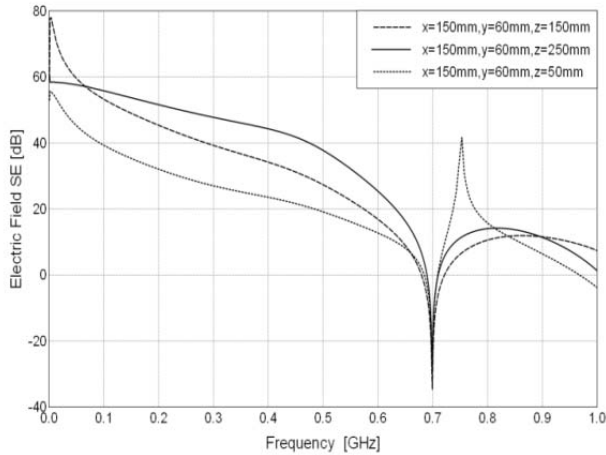


Fig 4 (a)

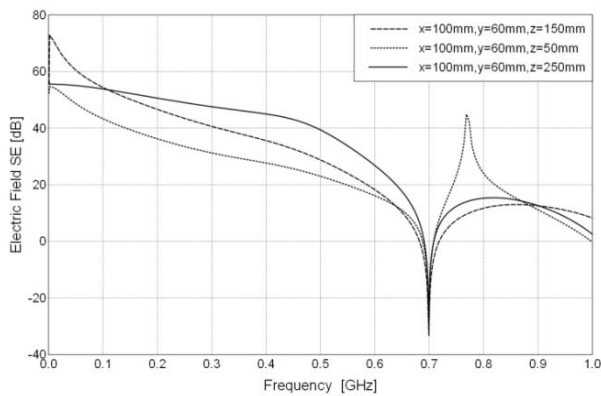


Fig 4 (b)

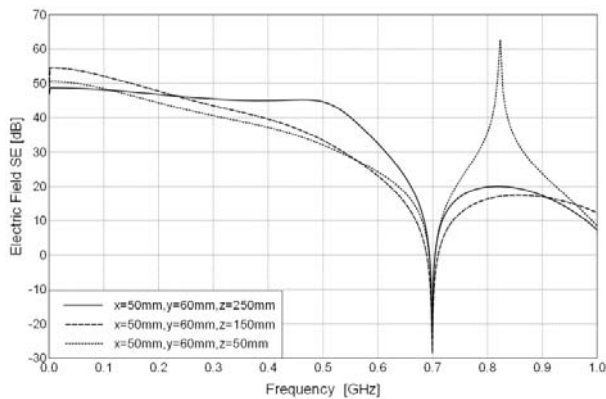


Fig 4 (c)

Figure 4 Electric field SE versus z value at different plane of 30cm×12cm×30cm enclosure with 10cm×0.5cm aperture located at 15cm×6cm in z=0 plane.

Shielding effectiveness at five different plane inside the enclosure obtained using the present method are plotted in Figure 4 which discuss electric field shielding effectiveness versus different z value. From the numerical data presented in Fig 4, it may be observed that electric field SE below the resonance frequency is influenced heavily by z value. Fig 4(a) and Fig 4(b) also show that the electric field SE increase rapidly to more than 40dB from 3dB at 0.75GHz on the z=50 plane, The electric field SE in Fig 4 (c) even reach 62dB at 0.82GHz. From what has been discussed above, it can be concluded that electric field SE is lower at the points near to the apertures than at larger distance from them, but when frequency exceed the resonance frequency, this result is wrong. Therefore low frequency sensitive apparatus inside the enclosure should be placed at the points far away from the apertures, which can improve the ability of electromagnetic compatibility.

Thirdly, we discuss electric field SE results calculated at three different points versus four square apertures having different arrays of position. We also consider 30cm×12cm×30cm enclosure with square apertures of size (4.0cm×4.0cm and 2cm×2cm). In Fig.5, there are one 4.0cm×4.0cm aperture located at 15cm×6cm and four 2cm×2cm apertures located at array 1((130,80,0) ,(130,40,0) ,(170,80,0) ,(170,40,0)), array 2((110,100,0) ,(190,100,0) ,(110,20,0) ,(190,20,0)), in z=0 plane.

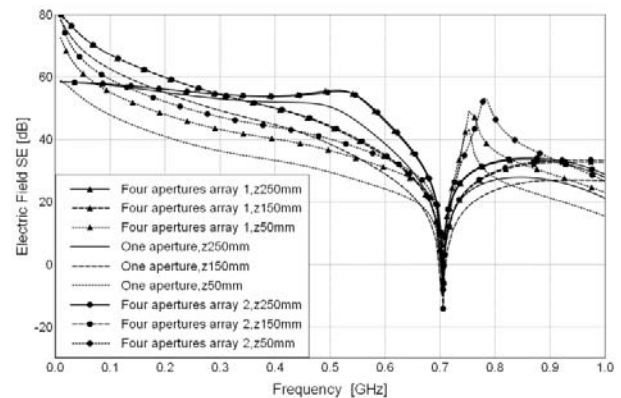


Figure 5. Electric field SE calculated at different points inside 30cm×12cm×30cm enclosure having a 4.0cm×4.0cm aperture located at 15cm×6cm, four 2.0cm×2.0cm apertures located at array 1 and array 2 in z=0 plane respectively illuminated by vertical polarized plane wave.

In Fig.5, it may be observed that the first resonance frequency is also about 0.7GHz, the maximum and minimum of electric field SE below the resonance frequency occur at z=250mm and z=50mm respectively, the maximum difference of electric field SE is about 20dB. It can also be concluded that lower electric field SE near the aperture than at location inside the enclosure farther away from the aperture, but when the frequency exceed the resonance frequency, this result is wrong. We also observe that the electric field SE have a similar changed trend at all frequency and the electric field SE of four apertures is higher

than that of one aperture while they have the same area. The results indicate that four apertures is a better select to improve the shielding ability of an enclosure than one aperture while they have the same area. We also note that there are little difference for different arrays for multiple apertures, which demonstrate that aperture's location array has little effect on the electric field SE.

IV. CONCLUSION

In this paper, an investigation on the effects of aperture' number and calculation point on electric field SE of metallic experiment box illuminated by vertical polarized plane waves has been carried out. For this purpose, modal MoM solution is formulated by employing surface equivalence principle and boundary conditions at each end of apertures. Numerical results on electric field SE are in good agreement with data available in the literature. The results indicate that apertures' position, aperture' number and calculation points have noticeable effect on the electric field SE. The simulation results also indicate that four apertures is a better select to improve the shielding ability of an enclosure than one aperture while they have the same area.

Acknowledgments

This work was supported by National Science funds of Civil Aviation Flight University of China(No. J2007-23)and Open Funds of CAAC academy of flight technology and safety.

REFERENCES

- [1] M. P. Robinson, J. D. Turner, D. W. P. Thomas, J. F. Dawson, M. D. Ganley, A. C. Marvin, S. J. Porter, T. M. Benson, and C. Christopoulos, "Shielding effectiveness of a rectangular enclosure with a rectangular aperture," *Electron. Lett.*, vol. 32, no. 17, 1996.
- [2] M. P. Robinson, T. M. Benson, C. Christopoulos, J. F. Dawson, M. D. Ganley, A. C. Marvin, S. J. Porter, and D. W. P. Thomas, "Analytical formulation for the shielding effectiveness of enclosures with apertures," *IEEE Trans. Electromagn. Compat.*, vol. 40, no. 3, pp. 240–248, Aug. 1998.
- [3] LIM., NUBEL J., DREWNIK J.L., HUBING T.H., DUBROFF R.E., VAN DOREN T.P.: 'EMI from cavity modes of shielding enclosures – FDTD modeling and measurements', *IEEE Trans. Electromagn. Compat.*, 2000, 42,(1), pp.29–38
- [4] M. Li, J. Nuebel, J. L. Drewniak, T. H. Hubing, R. E. DuBroff, and T.P. Van Doren, "EMI from cavity modes of shielding enclosures—FDTD modeling and measurements," *IEEE Trans. Electromagn. Compat.*, vol.42, no. 1, pp. 29–38, Feb. 2000.
- [5] BENHASSINE S., PICHON L., TABBARA W.: 'An efficient finite-element time-domain method for the analysis of the coupling between wave and shielded enclosure', *IEEE Trans. Magn.*, 2002, 38, (2), pp. 709–712.
- [6] W. P. Carpes Jr., L. Pinchon, and A. Razek, "Analysis of the coupling of an incident wave with a wire inside a cavity using an FEM in frequency and time domains," *IEEE Trans. Electromagn. Compat.*, vol. 44, no. 3, pp. 470–475, Aug. 2002.
- [7] WALLYN W., DE ZUTTER D., ROGIER H.: 'Prediction of the shielding and resonant behavior of multisection enclosures based on magnetic current modeling', *IEEE Trans. Electromagn. Compat.*, 2002, 44, (1), pp. 130–138
- [8] G. Wu, X.-G. Zhang, Z.-Q. Song, and B. Liu, "Analysis on Shielding Performance of Metallic Rectangular Cascaded Enclosure with Apertures," *Progress In Electromagnetics Research Letters*, Vol. 20, 185-195, 2011.
- [9] PODLOZNY V., CHRISTOPOULOS C., PAUL J.: 'Efficient description of fine features using digital filters in time domain computational electromagnetics', *IET Sci. Meas. Technol.*, 2002, 149, (5), pp. 254–257
- [10] R. Attari and K. Barkeshli, "Application of the transmission line matrix method to the calculation of the shielding effectiveness for metallic enclosures," in *Proc. IEEE Antennas Propagation Soc. Int. Symp.*, vol. 3, Jun. 16–21, 2002, pp. 302–305.
- [11] Wu,G.;Zhang,X.G.;Liu,B., "A Hybrid Method for Predicting the Shielding Effectiveness of Rectangular Metallic Enclosures with Thickness Apertures," *Journal of Electromagnetic Waves and Applications*, Volume 24, Numbers 8-9, 2010, pp.1157-1169(13).
- [12] Electromagnetic field penetration studies (NASA/CR-2000-210 297), M. D. Deshpande. (2000, Jun.). [Online]. Available: <http://techre-ports.larc.nasa.gov/ltrs/PDF/2000/cr/NASA-2000-cr210297.pdf>